

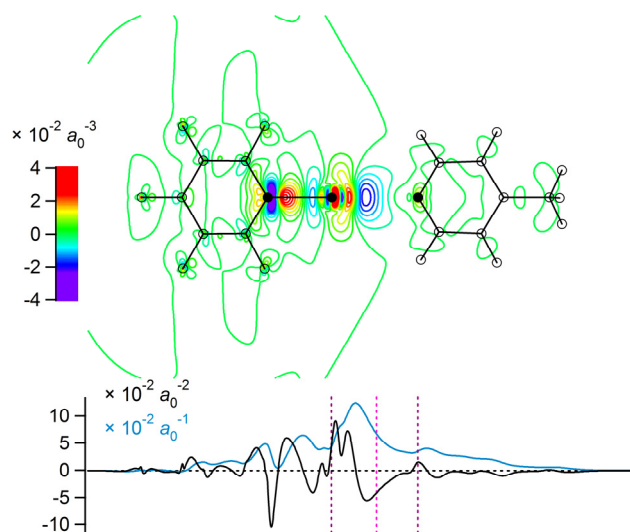
Supplementary Information

Correlation of the partial charge-transfer and covalent nature of halogen bonding with the THz and IR spectral changes

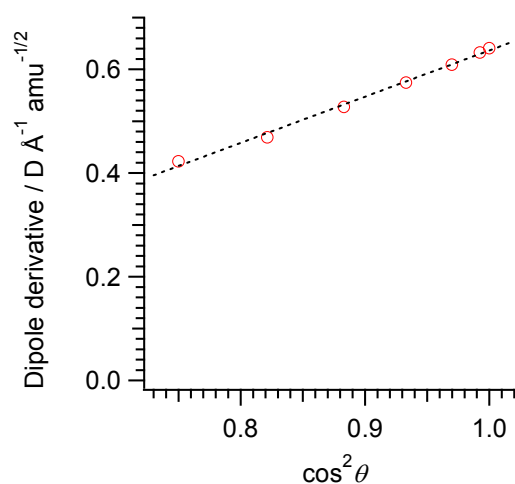
Hajime Torii*

Department of Applied Chemistry and Biochemical Engineering, Faculty of Engineering, and Department of Optoelectronics and Nanostructure Science, Graduate School of Science and Technology, Shizuoka University, 3-5-1 Johoku, Naka-ku, Hamamatsu 432-8561, Japan

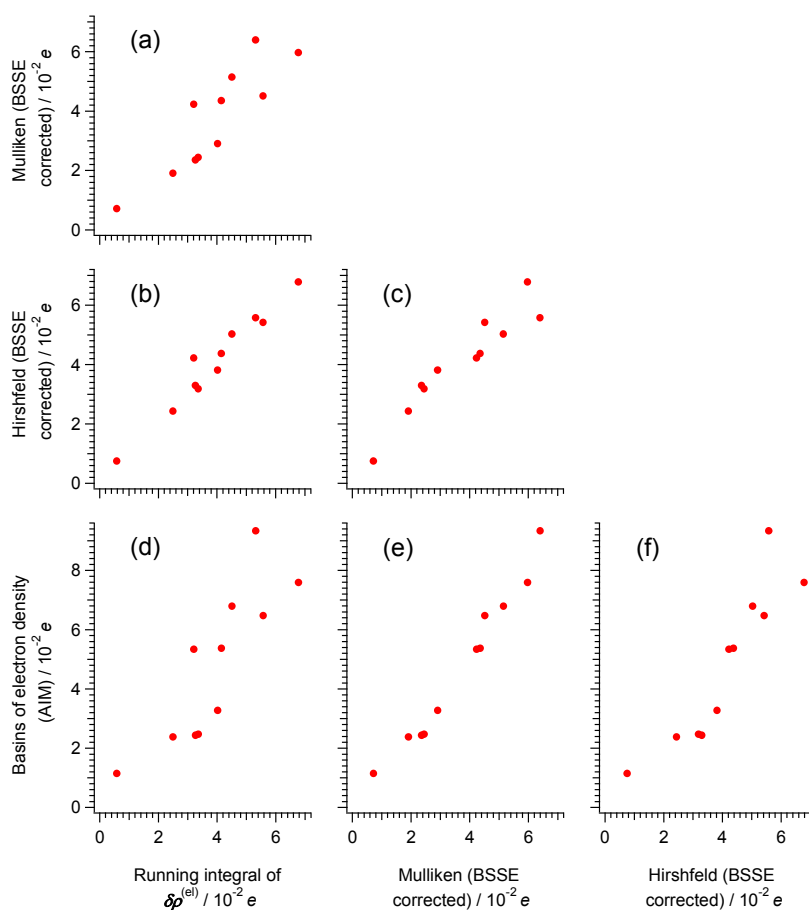
Supplementary Figures



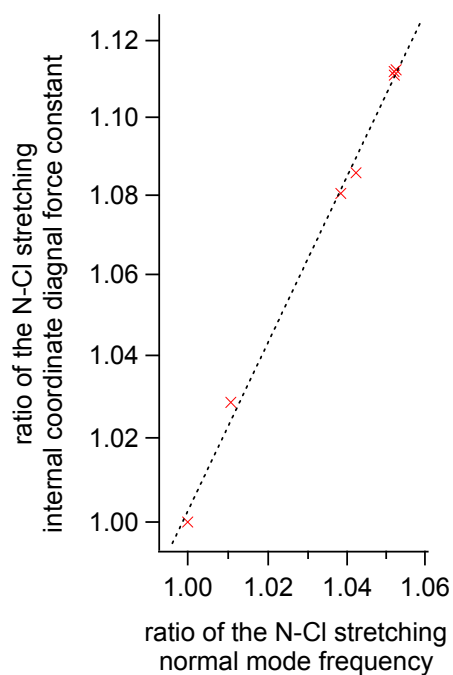
Fig, S1. Plots of the same type as Fig. 1 (b), but for the change in the electron density derivative occurring upon complex formation of the molecular translation of C₆F₅I along the *z* axis in the C₆F₅I...NC₅H₄CH₃ (4-methylpyridine) complex. The contours in the two-dimensional plot are drawn with the interval of $0.4 \times 10^{-2} a_0^{-3}$ in the range from $-10 \times 10^{-2} a_0^{-3}$ to $10 \times 10^{-2} a_0^{-3}$, with the colour code shown on the left-hand side. For comparison with the result for the C–I stretching mode shown in Fig. 1 (b), it should be noted that the vertical scale (which is weighted by the square root of the reduced atomic mass, i.e., $a_0^{-2} m_e^{-1/2}$ for the black curve and $a_0^{-1} m_e^{-1/2}$ for the light blue curve) used in the one-dimensional plot of Fig. 1 (b) should be multiplied by $6.36 \times 10^2 m_e^{1/2}$ (calculated from the real vibrational pattern of the mode) to be converted to the scale of the actual displacement (a_0^{-2} for the black curve and a_0^{-1} for the light blue curve), so that the charge flux calculated for the C–I stretching mode [Fig. 1 (b)] is a little larger than that calculated for the molecular translation of C₆F₅I (shown here).



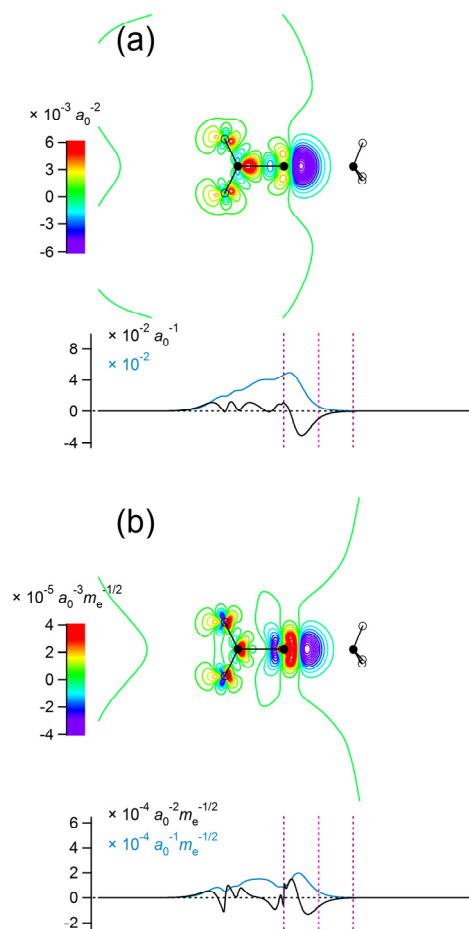
Fig, S2. Relation between the dipole derivative of the C–I stretching mode and the C–I...N angle (θ) calculated for the bent structures of the $\text{C}_6\text{F}_5\text{I}\cdots\text{NC}_5\text{H}_4\text{CH}_3$ (4-methylpyridine) complex.



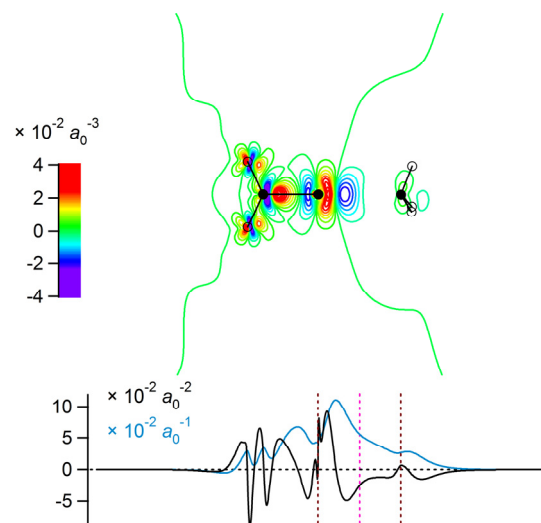
Fig, S3. Correlation among the extent of intermolecular charge transfer estimated from the running integral of $\delta[\rho^{(\text{el})}(\mathbf{r})]$, Mulliken and Hirshfeld population analyses (after correcting the BSSE), and the charges of the basins of electron density (called the AIM charges) calculated for the complexes of $\text{C}_6\text{F}_5\text{I}$ with trimethylamine, 4-methylpyridine, acetonitrile, trimethylphosphine, ethylidynephosphine, dimethylether, *N*-methylacetamide, dimethylthioether, and *N*-methylthioacetamide.



Fig, S4. Relation (log–log plot) between the ratios (with the values calculated for the isolated O_2NCl being taken as the reference) of the N–Cl stretching normal mode frequency and the N–Cl stretching internal coordinate diagonal force constant calculated for the complexes shown in Table 1. The black dotted line is a line of gradient 2 that is meant for the guide to the eye.

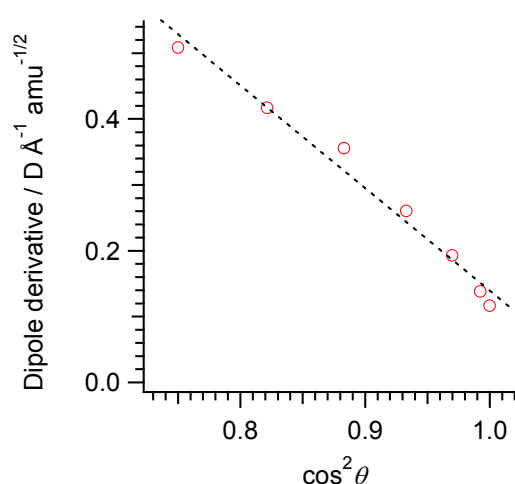


Fig, S5. Plots of the same type as Fig. 4, but calculated by replacing the NH_3 molecule with a set of CHelpG atomic charges in the $\text{O}_2\text{NCl}\cdots\text{NH}_3$ complex.



Fig, S6. Plots of the same type as Fig. 4 (b), but for the change in the electron density derivative occurring upon complex formation of the molecular translation of O_2NCl along the z axis in the $\text{O}_2\text{NCl}\cdots\text{NH}_3$ complex. The contours in the two-dimensional plot are drawn with the interval of $0.4 \times 10^{-2} a_0^{-3}$ in the range from $-10 \times 10^{-2} a_0^{-3}$ to $10 \times 10^{-2} a_0^{-3}$, with the colour code shown on the left-hand side.

For comparison with the result for the N–Cl stretching mode shown in Fig. 4 (b), it should be noted that the vertical scale (which is weighted by the square root of the reduced atomic mass, i.e., $a_0^{-2}m_e^{-1/2}$ for the black curve and $a_0^{-1}m_e^{-1/2}$ for the light blue curve) used in the one-dimensional plot of Fig. 4 (b) should be multiplied by $2.03 \times 10^2 m_e^{1/2}$ (calculated from the real vibrational pattern of the mode) to be converted to the scale of the actual displacement (a_0^{-2} for the black curve and a_0^{-1} for the light blue curve), so that the charge flux calculated for the N–Cl stretching mode [Fig. 4 (b)] is a little larger than that calculated for the molecular translation of O_2NCl (shown here).



Fig, S7. Relation between the dipole derivative of the N–Cl stretching mode and the N–Cl...N angle (θ) calculated for the bent structures of the $\text{O}_2\text{NCl}\cdots\text{NH}_3$ complex.

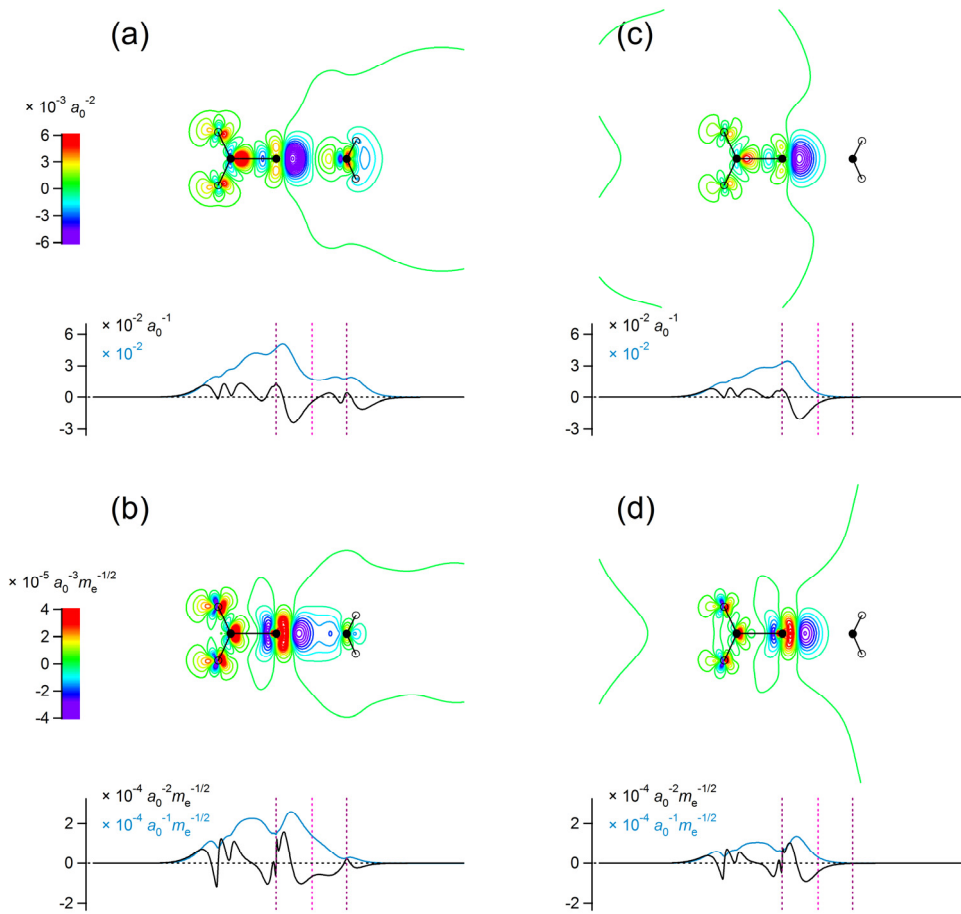


Fig. S8. (a,b) One- and two-dimensional plots depicted for $\delta[\rho^{(\text{el})}(\mathbf{r})]$ and $\delta[\partial\rho^{(\text{el})}(\mathbf{r})/\partial Q_{\text{NClstr}}]$ of the $\text{O}_2\text{NCl}\cdots\text{OH}_2$ complex. The contours in the two-dimensional plot are drawn in the same way as Fig. 4. (c,d) The plots of the same quantities but calculated by replacing the H_2O molecule with a set of CHelpG atomic charges.

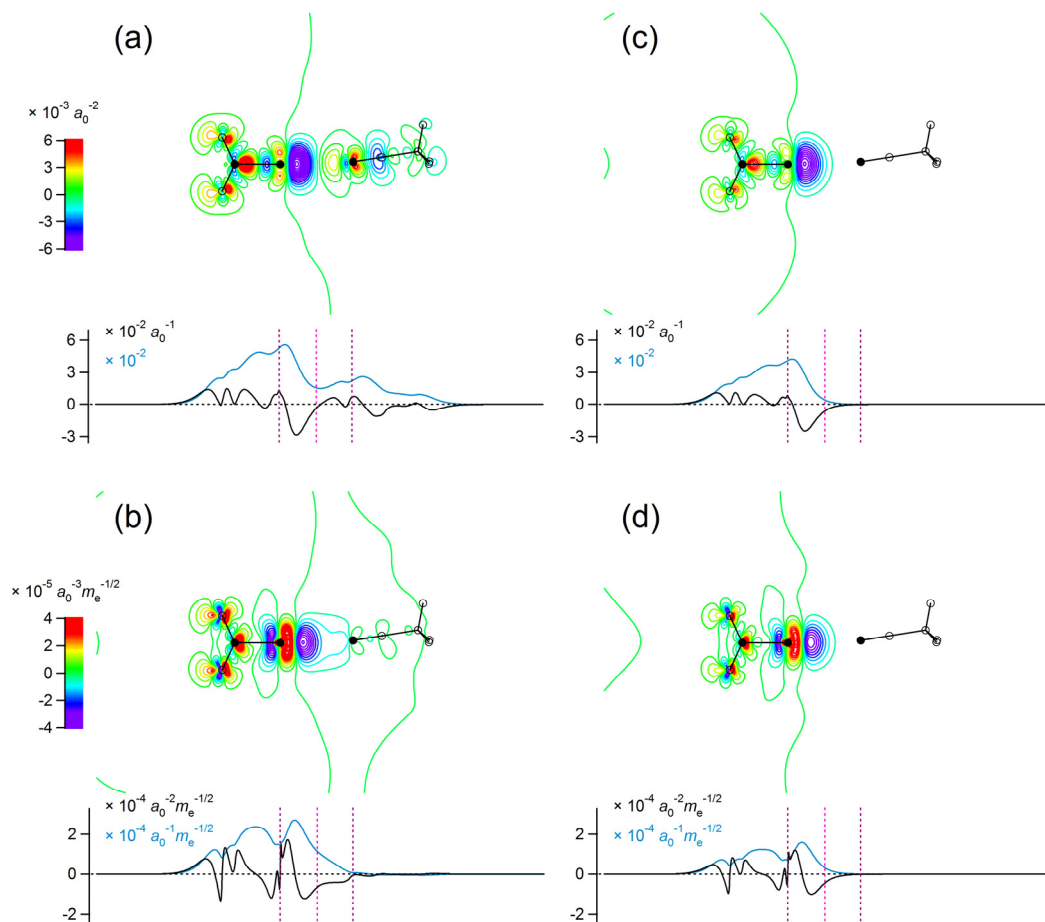


Fig. S9. (a,b) One- and two-dimensional plots depicted for $\delta[\rho^{(\text{el})}(\mathbf{r})]$ and $\delta[\partial\rho^{(\text{el})}(\mathbf{r})/\partial Q_{\text{NClstr}}]$ of the $\text{O}_2\text{NCl}\cdots\text{N}\equiv\text{CCH}_3$ complex. The contours in the two-dimensional plot are drawn in the same way as Fig. 4. (c,d) The plots of the same quantities but calculated by replacing the CH_3CN molecule with a set of CHelpG atomic charges.